Force Sensing Steerable Needle with Articulated Tip and Sensorized Tendons

Shivanand Pattanshetti*, Rohith Karthikeyan* and Seok Chang Ryu

Abstract— **This paper describes a unique design of tip-force sensing steerable needles (of size comparable to 17G and smaller), composed of a metal tube with laser-machined multi-DOF hinge joints near the tip, four force-sensing tendons actuating the joints, and multi-lumen polymer tubes guiding the tendons. For the feasibility test of the needle, a simple prototype using one sensorized and three other normal tendons was instrumented. The joint motions and force-sensing capability were investigated in air and within a tissue phantom and results were compared with those of another needle employing a flexure tip joint. Based on the promising initial results, we believe that the tip-force sensing needle with hinge joints represents a potentially highly attractive alternative to the existing flexure joint needles for minimally invasive interventions, especially where small needles and/or feedback features are indicated.**

I. INTRODUCTION

Most steerable needles or cannula investigated as part of surgical robotic instruments [1] comprised passive solid metal wires with sharp bevel tips [2], [3]. Typically, for a passive needle, a robot arm holds and manipulates the proximal end to send its distant tip to the site of interest, followed by the insertion of a flexible polymer sheath over the wire to create a working channel, a method known as the Seldinger technique [4]. Over the past decade, this passive needle steering approach has propelled surgical robotics into great success as an interventional modality and opened numerous new therapeutic applications that could not be readily implemented with more conventional laparoscopic techniques. However, several significant technical challenges remain in extending surgical robotics to more wide spread application areas, such as pediatric and neuro surgeries that demand smaller and smarter devices. Thus, as currently implemented, the indirect tip control approach requires a complicated mechanics model is to successfully operate inside inhomogeneous tissue, along with an external imaging modality such as CT or MRI, even for simple procedures. Furthermore, the Seldinger technique has not yet been validated within the highly frictional tissue environment for the advanced steerable needles proposed recently. It is also not clear whether a flexible tube channel is sturdy enough for performing advanced surgical tasks requiring accurate tip orientation control. It is therefore desirable to reevaluate the design of steerable needles and explore

Shivanand Pattanshetti, Rohith Karthikeyan and Seok Chang Ryu are with the BioRobotics Laboratory in the Department of Mechanical Engineering, Texas A&M University, College Station, TX 77843, USA shivanandvp, rohithkarthikeyan, scryu@tamu.edu

*Shivanand Pattanshetti and Rohith Karthikeyan contributed equally to this work.

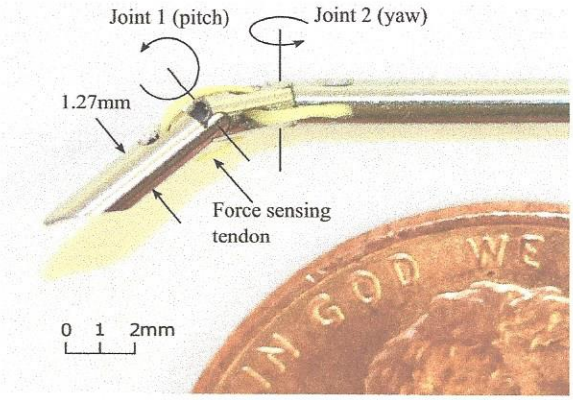

Fig. 1: Steerable needle prototype with orthogonally arranged two hinge joints near tip, composed of a 120 mm long and 1.27 mm outer diameter Nitinol tube and Kevlar connected optical fibers. Multi-lumen polymer tubes guiding tendons are omitted. The rotation range of each joint is designed to be $\pm 25°$.

innovative approaches that would allow extending the range of surgical applications that could be economically accessed with robotic instruments.

Recently, there have been a few pioneering studies on advanced needle-size device designs which explored, for example, laser machined flexure joint embedment on tubular structures [5], [6], functional improvements of the needle structure through either laser patterning [7] or negative Poissons ratio materials [8], and various innovative tip steerable needle designs [9], [10], [11], [12]. It is, however, generally acknowledged that new needle designs that would also allow introduction of reliable force-sensing and actuation modalities while creating a working channel for micro-scale flexible structures would be still more desirable, as expressed by an increasing number of surgeons [13].

A possible approach to addressing such a complex proposition, would be to integrate multiple functional components such as an actuator, a sensor and a joint, all within a single element. Accordingly, we introduce a unique tip-force sensing steerable needle design, as shown in Fig. 1, that employs two original robotic components: a polarization maintaining fiber Bragg gratings (PM-FBG)-based sensorized tendon for simultaneous actuation and tip-force sensing, and a tubular needle structure with laser-machined articulated tip that allows for tighter needle curvature than a comparable bent-tip needle [9]. The PM-FBG fiber enables separating the mechanical from thermal strain measurements, using a single sensing element, the FBG. The tubular structure with embedded hinge joints can then implement multi-DOF rotational joint motions at the tip location, while retaining a

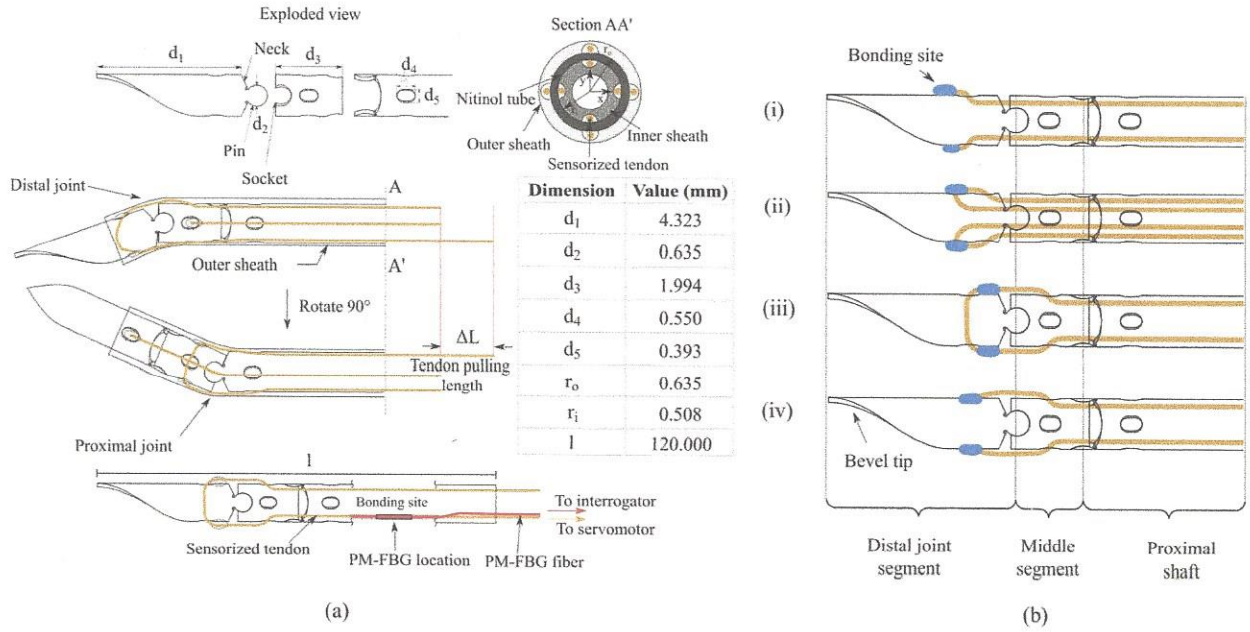

Fig. 2: Design and prototype of steerable needle. (a) exploded view depicting each segment (top), actuation configurations of the orthogonal hinges and dimensions (middle) and PM-FBG location (bottom). (b) various tendon routing methods. (iii) is selected in this paper for prototyping.

thin form factor and allowing for retaining a working channel within the tube.

The rest of this paper is organized as follows: In Section II, the design and prototype of the steerable needle are presented in detail, and the principle of PM-FBG is briefly introduced. In Section III, the tip joint motion actuated by the sensorized tendon is investigated in a tissue phantom as part of the feasibility study and the new needle performance is compared with that of a flexure joint needle, followed by conclusions and future work in Section IV.

II. Design and Needle Prototype

A. Tube with Laser-machined Hinge Joints

Steerable instruments in minimally invasive robotic surgery encompass at least 4 degrees of freedom (DOF), including pivoting in two perpendicular planes (pitch and yaw), axial rotation and translation from the proximal end [14]. To achieve the pitch and yaw motions, we incorporate two orthogonal hinge joints located near the distal end of the steerable needle, as shown in Fig. 2 (a). The tube segments that contain these hinges would then function like a universal joint.

The hinge joints are fabricated in-house using a 2 DOF Nd-YAG laser cutting machine (ProStent-1, Precision Automated Laser Systems, San Clemente, CA). The workpiece utilized is a 1.27 mm outer diameter Nitinol tube with a wall thickness of 0.127 mm. While cutting, the laser machine can rotate the workpiece about the tube axis as well as linearly translating it along the axis. Any design to be machined is prepared in a 2D planar sketch, on which toolpaths are generated. The laser machine cuts along these toolpaths, as though the sketch is radially wrapped around the cylinder. Hence, to fabricate the hinges, all 3D surface features on the tubular workpiece cast in the form:

$$z = f(x, y) \tag{1}$$

should be unwrapped into a two dimensional sketch,

$$\bar{y} = f\left[r_c.sin\left(\frac{\bar{x}}{r_c}\right), r_c.cos\left(\frac{\bar{x}}{r_c}\right)\right] \tag{2}$$

where x, y and z are 3D cartesian coordinates of the feature, while $\bar{x}$ and $\bar{y}$ are the mapped 2D cartesian coordinates of the feature for generating a toolpath and r_c is the radius of the cylindrical section on which the feature is to be cut.

Each hinge joint consists of three distinct features: *neck*, *pin* and *socket* (see Fig. 2 (a) top). Two segments of the tube mate together to form a hinge. One of these segments contains two diametrically opposite *necks*, jutting out from the rim of the tube and ending in two circular *pins*. The mating segment contains two hollow, circular *sockets* which enclose the *pins*. The 2 DOF machining described earlier creates opposing wedges between the two *pins* and *sockets* of the hinge, resulting in a hinge joint that does not dislodge diametrically [15]. The prototype that we use for testing consists of three segments - a distal segment with a bevel tip, a small middle segment, and a proximal segment with a long shaft for gripping. These segments have machined slots to allow for routing tendons that are used for actuation.

B. PM-FBG Fiber Tendons

As part of our design, we propose using a fiber-optically sensorized tendon actuation scheme because tendons can simplify the design and control of robotic needles, while offering a workaround to allow miniaturization as well as greater responsiveness, safety and flexibility features [16].

Furthermore, due to the proximity of the strain sensing FBG and the joint (Fig. 2 (a) bottom), the tension force transmitted to the joint, or external force on the joint, can be accurately estimated. A standard FBG, however, is sensitive to both mechanical and thermal strains, and although the latter could be compensated by placing additional fibers, this would increase the device size and limit design options. a PM-FBG fiber offers a solution to this coupling issue. Such PM fibers are usually fabricated by introducing stress-induced linear birefringence into the fiber structure. This preserves the polarization state of the transmitted wavelength, provided the light path is aligned with either axis of birefringence. For this, as shown in Fig. 3 (a), a single PM-FBG has double Bragg reflection peaks at any given instant.

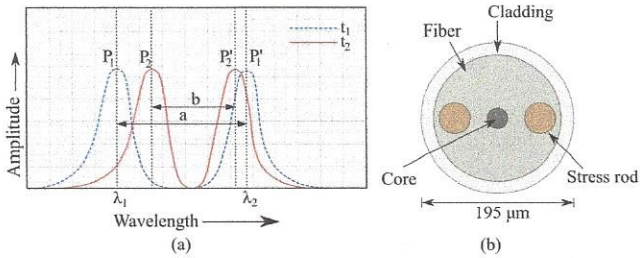

Fig. 3: Spectral response (a) and cross sectional view (b) of a single PM-FBG fiber. The instantaneous peak separation (a at time t_1 and b at time t_2) relates to temperature, while their temporal difference is proportional to fiber strain.

The response of the dual wavelength spectra to temperature and strain is similar to that of a standard non-PM-FBG. However, the sensitivities of individual peaks differ. The two plots shown in Fig. 3 represent the results of consecutive sampling instances at time t_1 and t_2. Here, a represents peak separation at time instant t_1 while the peak separation is b at time t_2. Calibration studies indicate that the separation between peaks P1 and P1' corresponds to temperature fluctuations while the mechanical strain can be inferred from the relative change in peak wavelengths [17]. Accordingly, the decoupled temperature change ΔT and mechanical strain change $\Delta\epsilon$ can be expressed as,

$$\Delta T = A\Delta\lambda_1 - B\Delta\lambda_2$$
$$\Delta\epsilon = C\Delta\lambda_1 - D\Delta\lambda_2 \quad (3)$$

where $\Delta\lambda_1$ and $\Delta\lambda_2$ are the changes of peak wavelengths with respect to a reference wavelength at known temperature and strain values, with the respective sensitivity parameters A, B, C, and D for ϵ and T derived empirically.

For this work, only one tendon out of the four was sensorized by bonding a bare 195 μm PM-FBG fiber (FBGS Technologies GmbH, Jena, Germany) to a pre-tensioned 125 μm Kevlar fiber bundle, using an instant adhesive (Loctite 403, Henkel Adhesives, USA), and tethered to the distal joint. The bonding length of about 20 mm was cured for 24 hours and located just behind the joints. The Kevlar reinforcement enabled higher tensile load transmission features and allowed for unique tethering configurations that are advantageous to the specific needle application.

C. Sensorized Tendon Routing

Various tendon routing methods, shown in Fig. 2 (b), were considered for our prototype. In Method (i), the tendon runs obliquely near the attachment point. This, however, was found to decrease the generated moment about the joint for a given tendon force. Method (ii) also had the same disadvantage, but could exert higher forces as there are two strands of tendons for each direction of joint motion. Methods (iii) and (iv) both offer a larger moment with (iv) being the preferred configuration. However, we used method (iii) to build the prototype described in this paper because it allowed for easier bonding and routing of the Kevlar-FBG composite inside the tube by just pulling the other end of the tendon.

III. Experiments and Results

The proximal ends of the four tendons were secured to pulleys attached to servomotors on the test setup shown in

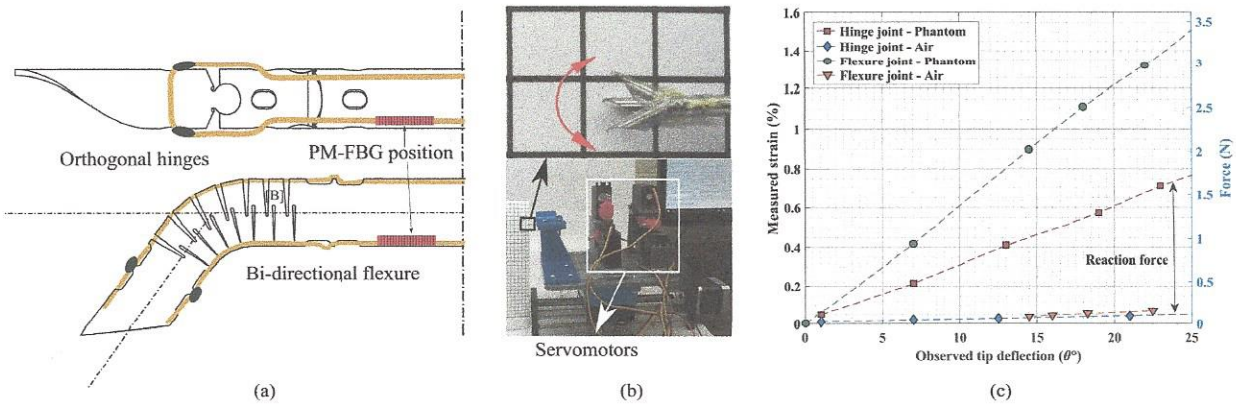

Fig. 4: Experiment setup and results. (a) two different joint types (hinge and flexure) of needles tested. (b) bent joint in air (top) and experimental setup (bottom). (c) strain and corresponding force measured by the sensorized tendon at various tip angles.

Fig. 4 (b). The sensorized tendon's optical fiber is connected to a tunable laser interrogator (FAZ Technologies, Dublin, Ireland) which delivers pulses of light and processes the return signals. The sensing data acquired by the interrogator are computer processed to yield strain and temperature change of the Kevlar-PM FBG composite. Since this structure is close to the distal bevel tip, it can be used to measure tip forces exerted on the needle by surrounding tissue.

The needle prototype is attached to a 3D printed clutch installed on the actuation system that consists of a linear ball-screw slide, servomotors, driving circuitry and a computer system. The four servomotors are fitted with pulleys that have screws to anchor tendons in place for tensioning. These servomotors are suitably oriented and affixed onto the movable platform such that all tendons can be directed from the pulleys to the proximal end of the needle. A custom designed computer program with on-screen controls is used to precisely control the action of the servomotors and the linear slide. Tissue phantoms used in the experiment comprised medical grade ballistic gels (Medical Grade 2, Clear Ballistics Inc., Fort Smith, AR). These were confirmed to have an elastic modulus of 42.1 kPa using bench-top compression testing equipment.

To evaluate the force sensing capability of the proposed needle, the distal joint was actuated by pulling a sensorized tendon in two different environments, air and tissue phantom. The force difference between the two cases is attributed to the tissue reaction force. With reasonable assumptions about the tissue deformation behavior, the strain response lends itself directly to tissue stiffness estimation. The same tests were repeated with a planar flexure joint needle using the routing Method (i) (see Fig. 4 (a) bottom) for comparison. Fig. 4 (c) demonstrates the strain and force responses of the two different needles in the two different environments. The plot shown represents the average of three consistent trials, with the strains processed using a low-pass filter to account for induced and ambient mechanical noise.

The elongation of both tendons is relatively low (less than 2 % strain) up to the designed range of joint rotation, enabling us to reasonably separate the joint kinematics from the tip-force estimation. In other words, the joint angle is independently measured by only the tendon pulling length, while the tip force is measured only by the PM-FBG signal. The slopes of the two needles, however, differ from each other. Although further investigation is necessary, the proposed hinge joint needle experiences about one half tissue reaction force as compared to the flexure joint needle to reach a comparable tip angle, partially attributed to the shorter tip lengths and improved rounting. The hinge joint force sensing needle would therefore appear to be a promising potential alternative to the existing flexure joint needles for minimally invasive intervention.

IV. Conclusions and Future Work

We demonstrated the feasibility of an articulate robotic needle design where laser-machined orthogonal hinge joints permit tip-steering, while Kevlar reinforced PM-FBG fibers enable force-estimation. The needle prototype had a geometric range of $\pm 25^\circ$ in tip deflection, but could extend further due to bending effects. The difference between the strain measured when in air and when within phantom, provides an estimate of the reaction force component generated by tissue, indicating a fairly linear trend. Further, the approach of embedding laser machined hinge joints can spatially accommodate an inner channel for drug delivery, allowing for ready customization, and while eliminating the need for micro assembly. Concurrently, the Kevlar reinforced PM-FBG fibers can provide means for haptic feedback through localized force and stiffness estimation and friction modeling.

In the future, we will test the steerability of standard size needles in tissue phantoms and perform combined insertion and tip actuation tests to reach specified targets. We will also conduct experiments using an outer multi-lumen tube to guide these tendons, to keep the pin in place, and to strengthen the joint against buckling. The kinematics of the tendon will then be determined with greater certainty as an aid in implementing precise control and estimation of the tips position. Finally, whereas the work described in this paper focused on a steerable needle, we note that several of the key components inherent to the design would be applicable to various robotic devices such as biomimetic micro-robot limbs, tendon-based actuation of robotic hands and existing micro surgical robotic tools.

References

[1] S. P. DiMaio and S. Salcudean, "Needle steering and motion planning in soft tissues," *IEEE Transactions on Biomedical Engineering*, vol. 52, no. 6, pp. 965–974, 2005.

[2] R. J. Webster, J. S. Kim, N. J. Cowan, G. S. Chirikjian, and A. M. Okamura, "Nonholonomic modeling of needle steering," *The International Journal of Robotics Research*, vol. 25, no. 5-6, pp. 509–525, 2006.

[3] S. Misra, K. B. Reed, B. W. Schafer, K. Ramesh, and A. M. Okamura, "Mechanics of flexible needles robotically steered through soft tissue," *The International Journal of Robotics Research*, 2010.

[4] S. I. Seldinger, "Catheter replacement of the needle in percutaneous arteriography: a new technique," *Acta radiologica*, vol. 39, no. 5, pp. 368–376, 1953.

[5] S. C. Ryu, Z. F. Quek, J.-S. Koh, P. Renaud, R. J. Black, B. Moslehi, B. L. Daniel, K.-J. Cho, and M. R. Cutkosky, "Design of an optically controlled mr-compatible active needle," *IEEE Transactions on Robotics*, vol. 31, no. 1, pp. 1–11, 2015.

[6] P. A. York, P. J. Swaney, H. B. Gilbert, and R. J. Webster, "A wrist for needle-sized surgical robots," in *IEEE International Conference on Robotics and Automation*, pp. 1776–1781, IEEE, 2015.

[7] D.-Y. Lee, J. Kim, J.-S. Kim, C. Baek, G. Noh, D.-N. Kim, K. Kim, S. Kang, and K.-J. Cho, "Anisotropic patterning to reduce instability of concentric-tube robots," *IEEE Transactions on Robotics*, vol. 31, no. 6, pp. 1311–1323, 2015.

[8] S. C. Ryu and P. E. Dupont, "Fbg-based shape sensing tubes for continuum robots," in *IEEE International Conference on Robotics and Automation*, pp. 3531–3537, IEEE, 2014.

[9] T. K. Adebar, J. D. Greer, P. F. Laeseke, G. L. Hwang, and A. M. Okamura, "Methods for improving the curvature of steerable needles in biological tissue," *IEEE Transactions on Biomedical Engineering*, vol. 63, no. 6, pp. 1167–1177, 2016.

[10] P. J. Swaney, J. Burgner, H. B. Gilbert, and R. J. Webster, "A flexure-based steerable needle: high curvature with reduced tissue damage," *IEEE Transactions on Biomedical Engineering*, vol. 60, no. 4, pp. 906–909, 2013.

[11] N. Shahriari, R. J. Roesthuis, N. J. van de Berg, J. J. van den Dobbelsteen, and S. Misra, "Steering an actuated-tip needle in biological tissue: Fusing fbg-sensor data and ultrasound images," in *IEEE International Conference on Robotics and Automation*, pp. 4443–4449, IEEE, 2016.

[12] A. J. Petruska, F. Ruetz, A. Hong, L. Regli, O. Sürücü, A. Zemmar, and B. J. Nelson, "Magnetic needle guidance for neurosurgery: Initial design and proof of concept," in *IEEE International Conference on Robotics and Automation*, pp. 4392–4397, IEEE, 2016.

[13] A. Trejos, R. Patel, and M. Naish, "Force sensing and its application in minimally invasive surgery and therapy: a survey," *Proceedings of the Institution of Mechanical Engineers, Part C: Journal of Mechanical Engineering Science*, vol. 224, no. 7, pp. 1435–1454, 2010.

[14] F. Jelínek, E. A. Arkenbout, P. W. Henselmans, R. Pessers, and P. Breedveld, "Classification of joints used in steerable instruments for minimally invasive surgerya review of the state of the art," *Journal of Medical Devices*, vol. 9, no. 1, p. 010801, 2015.

[15] R. D. Brunnen and T. J. Simon, "Bendable portion of an insertion tube of an endoscope and method of producing it," Aug. 3 2010. US Patent 7,766,821.

[16] H. M. Le, T. N. Do, and S. J. Phee, "A survey on actuators-driven surgical robots," *Sensors and Actuators A: Physical*, 2016.

[17] S. K. Ibrahim, M. Farnan, D. M. Karabacak, and J. M. Singer, "Enabling technologies for fiber optic sensing," in *SPIE Photonics Europe*, pp. 98990Z–98990Z, International Society for Optics and Photonics, 2016.